Analytical Biochemistry 442 (2013) 231–236

Contents lists available at ScienceDirect

Analytical Biochemistry

journal homepage: www.elsevier.com/locate/yabio

Quantitative affinity electrophoresis of RNA–small molecule interactions by cross-linking the ligand to acrylamide

Sherry N. Boodram, Lucas C. McCann, Michael G. Organ, Philip E. Johnson *

Department of Chemistry, York University, Toronto, Ontario M3J 1P3, Canada

ARTICLE INFO

Article history:
Received 11 June 2013
Received in revised form 27 July 2013
Accepted 29 July 2013
Available online 6 August 2013

Keywords:
Affinity electrophoresis
RNA–small molecule interactions
Aminoglycosides

ABSTRACT

We show that the affinity electrophoresis analysis of RNA–small molecule interactions can be made quantifiable by cross-linking the ligand to the gel matrix. Using an RNA–aminoglycoside model system to verify our method, we attached an acryloyl chloride molecule to the aminoglycosides paromomycin and neomycin B to synthesize an acrylamide–aminoglycoside monomer. This molecule was then used as a component in gel polymerization for affinity electrophoresis, covalently attaching an aminoglycoside molecule to the gel matrix. To test RNA binding to the cross-linked aminoglycosides, we used the aminoglycoside binding RNA molecule derived from thymidylate synthase messenger RNA (mRNA) that contains a C–C mismatch. Binding is indicated by the difference in RNA mobility between gels with cross-linked ligand, with ligand embedded during polymerization, and with no ligand present. Critically, the predicted straight line relationship between the reciprocal of the relative migration of the RNA and the ligand concentration is obtained when using cross-linked aminoglycosides, whereas a straight line is not obtained using embedded aminoglycosides. Average apparent dissociation constants are determined from the slope of the line from these plots. This method allows an easy quantitative comparison between different nucleic acid molecules for a small molecule ligand.

The ability of RNA to interact with small molecules is the basis for a wide assortment of biochemical functions. In nature RNA–small molecule interactions in riboswitches regulate gene expression [1,2], whereas in biotechnology applications RNA aptamers can be selected as biosensors for small molecules [3]. In addition, the interactions between RNA and small molecules govern the action of a number of medicinally important molecules such as the aminoglycoside class of antibiotics (Fig. 1) [4,5]. The chemical and structural diversity of antibiotics makes these molecules particularly interesting for understanding the binding specificity of RNA for its target ligands [6–9]. Aside from its interactions with small molecules, RNA has many other important functions in cellular processes [10–12]. Controlling the biological function of RNA through the binding of a small molecule would be a powerful biochemical tool. For this reason, developing a method of quickly and easily identifying compounds that bind to RNA of a defined size or shape would be very beneficial.

There are many biophysical methods available to study RNA–small molecule interactions, including isothermal titration calorimetry (ITC),[1] surface plasmon resonance (SPR), and fluorescence anisotropy. In addition, a microfluidic-based method that measures the affinity of a riboswitch for a ligand was reported recently [13]. However, many of these techniques require specialized and expensive equipment. Although the interaction of RNA with proteins is often readily investigated using a simple electrophoretic mobility shift assay (EMSA) or gel shift assay [14,15], this technique is limited when applied to RNA–small molecule systems because of the negligible difference in mobility between free and bound RNA. An alternate gel-based method for determining binding affinity is affinity electrophoresis. Several examples that detect the binding of molecules using affinity electrophoresis have been published, although in each case this technique has been limited to interactions involving proteins or peptides with another molecule [16–21].

Previously, we showed that affinity electrophoresis can be used to detect RNA–small molecule interactions [22]. In this method, the acrylamide gel is polymerized in the absence and presence of ligand such that the ligand is embedded into the gel matrix during polymerization. The RNA molecule is then run through the gel, and binding is gauged by the difference in mobility of the bands between the gels polymerized with and without ligand. As a control, mobility is also compared with a nonbinding internal standard. Although this method can identify interactions between small molecules and RNA, the binding is not easily quantifiable because the small molecule ligand can move in the gel during

* Corresponding author. Fax: +1 416 736 5936.
E-mail address: pjohnson@yorku.ca (P.E. Johnson).

[1] *Abbreviations used:* ITC, isothermal titration calorimetry; mRNA, messenger RNA; TSMC, thymidylate synthase mRNA; ddH_2O, double distilled water; EDTA, ethylenediaminetetraacetic acid; TBE, Tris–borate–EDTA; IR, infrared; HRMS, high-resolution mass spectrometry.

0003-2697/$ - see front matter © 2013 Elsevier Inc. All rights reserved.
http://dx.doi.org/10.1016/j.ab.2013.07.040

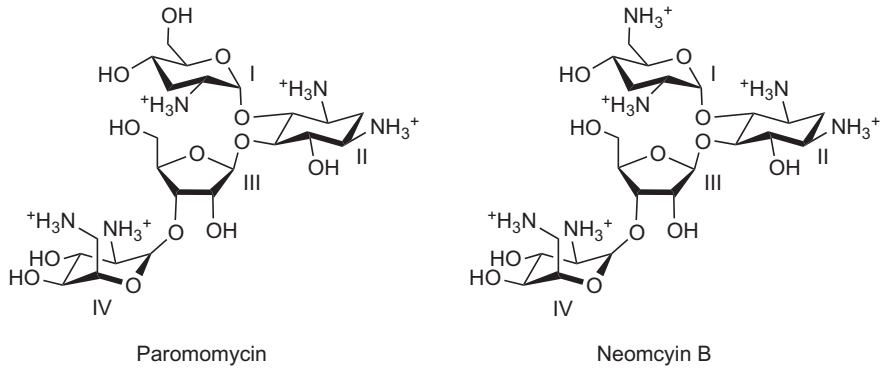

Fig.1. Chemical structure of the aminoglycoside molecules paromomycin and neomycin B.

electrophoresis. For the ligand to be stationary during electrophoresis, it must be either uncharged or too large to move through the gel. Aminoglycosides are neither.

Here, we modified our affinity electrophoresis method to make the technique quantifiable for RNA–small molecule interactions. We chemically modified the aminoglycoside by attaching an acrylamide monomer onto the structure. We then added this modified aminoglycoside to the acrylamide mixture during polymerization, with the result being that the ligand becomes covalently attached to the gel and cannot move during electrophoresis. By measuring the relative migration values (R_r) and plotting $1/R_r$ versus ligand concentration, we obtained a straight line from which an average apparent K_d can be determined.

Materials and methods

RNA preparation

The thymidylate synthase mRNA (TSMC) sample (Fig. 2) was prepared by *in vitro* transcription [23] in a manner described previously [22,24].

Synthesis of cross-linked aminoglycoside–acrylamide

In a flame-dried vial containing a stirrer, aminoglycoside sulfate salt (0.5 mmol, 1.0 equiv) was added before it was sealed with a septum. The vial was purged under high-vacuum and backfilled with Ar (g) three times before a distilled deionized water (ddH_2O) solution (totaling 1 ml) containing Na_2CO_3 (46 mg, 0.55 mmol, 1.1 equiv) was added via syringe. The resultant suspension was sonicated for 5 min until the mixture was solubilized completely. To the clear yellow solution was added acryloyl chloride (50 μl, 0.55 mmol, 1.1 equiv) in one portion via microliter syringe. The resultant solution was left to stir at room temperature for 24 h and was carried forward for polymerization reactions without further purification.

Affinity gel electrophoresis

For both the cross-linked and embedded gel preparations, 20% (m/v) polyacrylamide (19:1 acrylamide/bisacrylamide) nondenaturing electrophoresis gels of the TSMC RNA were run along with a control gel containing varying amounts of the appropriate aminoglycosides paromomycin and neomycin B (Sigma–Aldrich). Gels were prepared using the Bio-Rad Mini-PROTEAN 3 apparatus with a 10 cm × 7.5 cm × 0.75-mm gel. All gels were run in a 0.5× Tris–borate–EDTA (TBE) buffer (1× TBE: 9 mM Tris, 9 mM boric acid, and 0.3 mM EDTA) at room temperature for 30 min at 300 V using the constant current setting. Bromophenol blue/xylene cyanol (blue/green dye) was run as an internal standard. RNA was detected using Stains-All (Sigma–Aldrich). In each lane, 1 μl of an RNA solution was loaded. The RNA solution was composed of a 1:1 mixture of 0.13 mM TSMC RNA/50% glycerol (v/v).

The affinity electrophoresis gels were analyzed according to the method of Takeo [17] to quantify the average apparent binding affinity. This method is summarized here. For the equilibrium between a macromolecule (M) and a ligand (L),

$$M + L \leftrightarrows ML. \tag{1}$$

The apparent dissociation constant is given by Eq. (2):

$$K_d = \frac{[M][L]}{[ML]}. \tag{2}$$

If the distance migrated by the macromolecule in the absence of ligand is given by R_o and the distance migrated in the presence of a particular concentration of ligand is r, then:

Fig.2. Sequence and secondary structure of the aminoglycoside binding RNA molecule used in this study. It is derived from thymidylate synthase mRNA (TSMC) and contains a C–C mismatch.

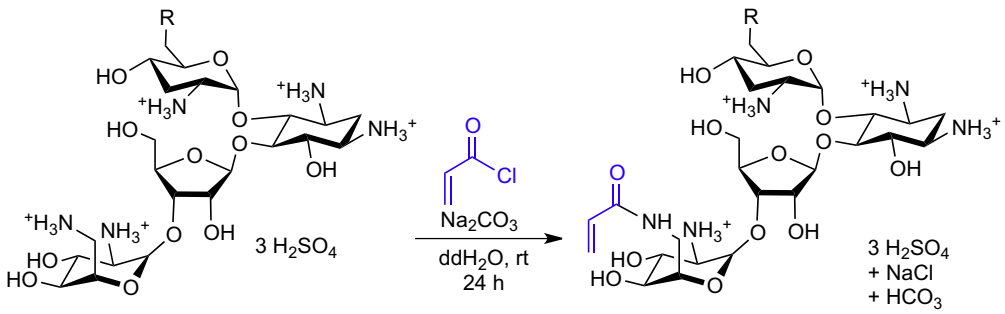

Fig.3. Reaction scheme for cross-linked acrylamide–paromomycin and acrylamide–neomycin B when R=OH and R=NH_3^+, respectively. One product is shown from a potential range of cross-linked acrylamide products.

$$\frac{R_o}{r} = \frac{[M]_t}{[M]} = \frac{[ML]+[M]}{[M]} = \frac{[ML]}{[M]} + 1, \quad (3)$$

where $[M]_t$ is the total concentration of the macromolecule. If Eq. (2) is rearranged and substituted into Eq. (3), then:

$$\frac{R_o}{r} = \frac{[L]}{K_d} + 1. \quad (4)$$

In our graphs, we define the relative migration R_r as:

$$R_r = \frac{r}{R_o}. \quad (5)$$

Therefore, Eq. (4) becomes:

$$\frac{1}{R_r} = \frac{[L]}{K_d} + 1. \quad (6)$$

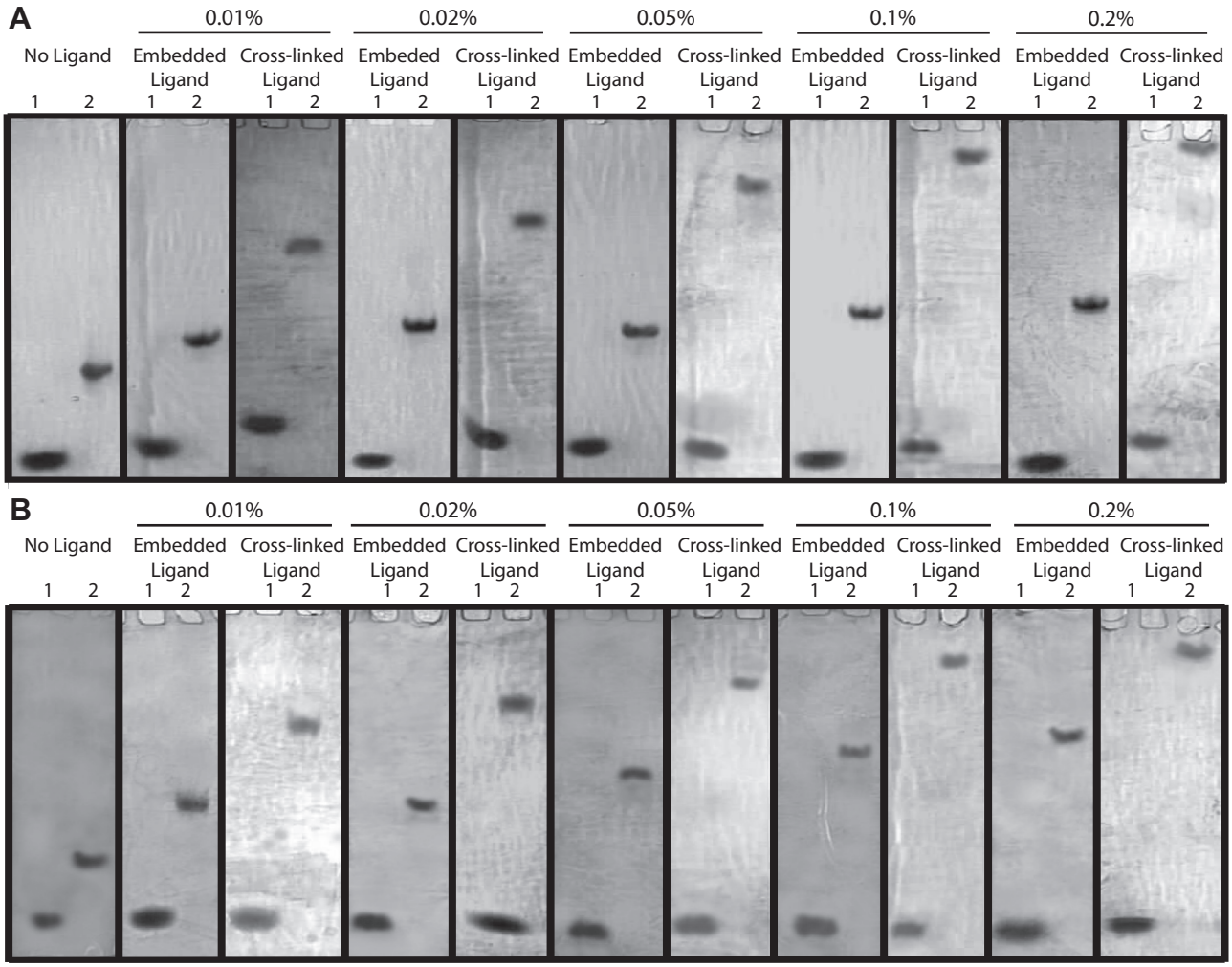

Fig.4. Affinity electrophoresis demonstrating the difference in mobility of the TSMC RNA between embedded and cross-linked paromomycin (A) and cross-linked neomycin B (B). Shown are separate gels containing different concentrations of ligand when copolymerized within the gel matrix (embedded) versus when the ligand is cross-linked to the gel matrix. Compared with the gels with embedded aminoglycoside, decreased mobility of the TSMC RNA is observed when the ligand is cross-linked to the gel matrix. Shown are 20% (m/v) polyacrylamide gels containing 0%, 0.01%, 0.02%, 0.05%, 0.1%, and 0.2% (m/v) ligand (embedded and cross-linked). In each gel, lane 1 is the bromophenol blue internal standard and lane 2 contains the TSMC RNA.

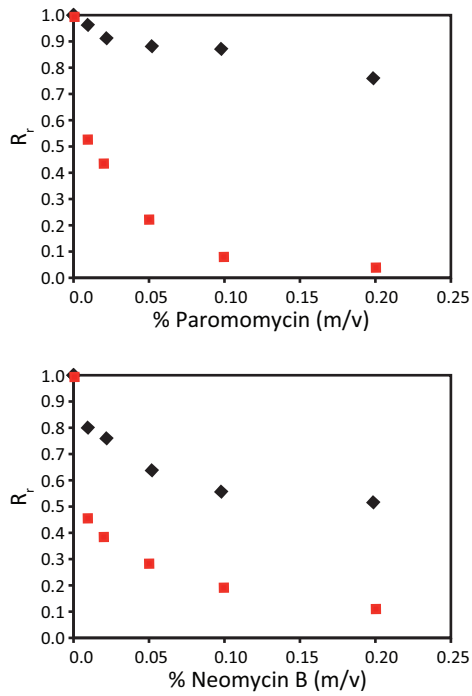

Fig.5. Plots comparing the relative migration (R_r) between TSMC RNA interacting with the cross-linked paromomycin and cross-linked neomycin B (red squares) and TSMC RNA interacting with the embedded paromomycin and embedded neomycin B (black diamonds). (For interpretation of the references to color in this figure legend, the reader is referred to the Web version of this article.)

A plot of $\frac{1}{R_r}$ versus $[L]$ will give a straight line with a slope of $\frac{1}{K_d}$ under conditions where the total concentration of the ligand (L) is much greater than the total concentration of macromolecule.

Results

To prevent the aminoglycoside ligand from moving in the gel during electrophoresis, paromomycin and neomycin B aminoglycosides were reacted with acryloyl chloride to form an acrylamide–aminoglycoside (Fig. 3). Formation of the acrylamide–aminoglycoside is straightforward. With the conditions used, there is on average one acrylamide added per aminoglycoside molecule. However, there is no control over the location of the acrylamide monomer, and the acryloyl chloride could react with any of the amine or alcohol groups on the aminoglycoside. A mixture of acrylamide–aminoglycoside products that differ by the location of the acrylamide monomer is produced.

Confirmation of acrylamide–aminoglycoside synthesis was made by infrared (IR) and high-resolution mass spectrometry (HRMS). ^{1}H and ^{13}C nuclear magnetic resonance (NMR) was also performed on the products in D_2O; however, these results were inconclusive due to extensive peak overlap. IR spectra indicate a loss of the O–H stretch and N–H stretch for both cross-linked acrylamide–aminoglycosides compared with the free aminoglycosides. This loss of the O–H stretch and N–H stretch suggests that the acryloyl chloride is reacting with both the alcohol and amine groups on the aminoglycoside. HRMS provided exact molecular weights of the expected acrylamide–aminoglycoside products. The theoretical value for neomycin B is 637.3170, and the determined value is 637.3170. For paromomycin, the theoretical value is 638.3010, and the determined value is 638.3015. Because it was only necessary that the acrylamide monomer be attached to the aminoglycoside, purification and isolation of the cross-linked acrylamide–aminoglycoside was not required. As a result, yields were not determined.

Cross-linking of the acrylamide–aminoglycoside was performed by adding the required amount of the acrylamide–aminoglycoside for a particular mass/volume percentage to the acrylamide mixture prior to adding the tetramethylethylenedi-

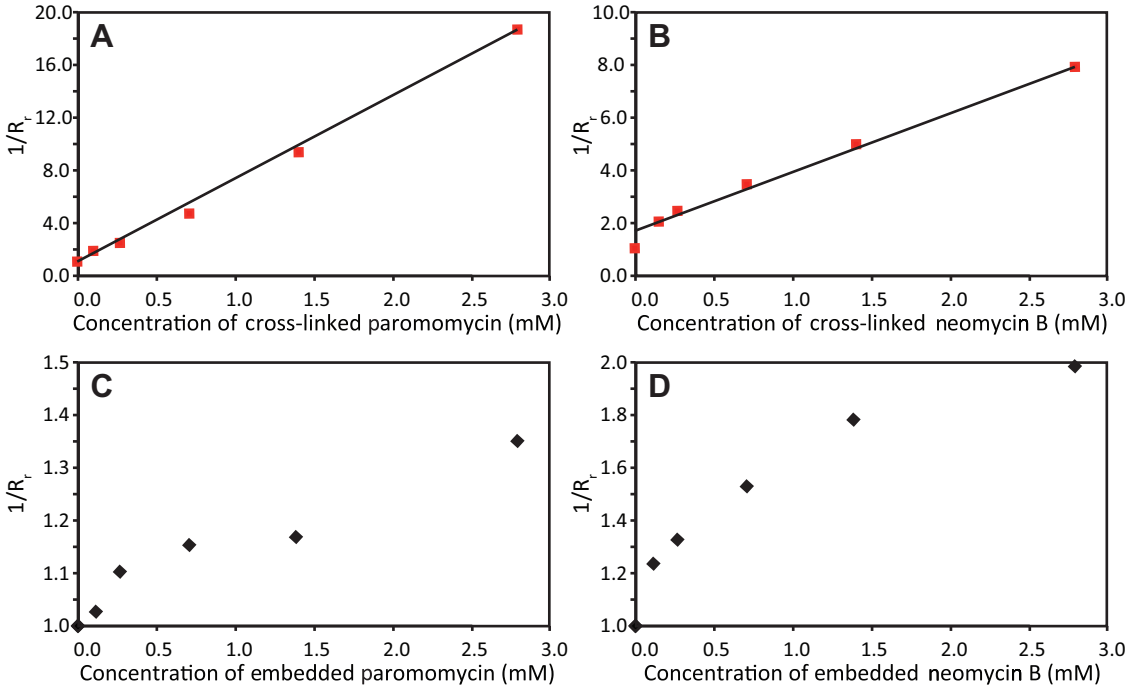

Fig.6. Plots showing the quantitative binding between cross-linked aminoglycosides and the TSMC RNA. Binding affinity is determined from the slope of the straight line given by the plot of the reciprocal of the relative migration ($1/R_r$) of TSMC RNA versus ligand concentration of cross-linked paromomycin (A) and cross-linked neomycin B (B). In comparison, plots of the embedded paromomycin (C) and embedded neomycin B (D) do not result in a straight line.

amine (TEMED) and ammonium persulfate (APS) polymerizing agents. Affinity gel electrophoresis was performed using either cross-linked ligands of acrylamide paromomycin or acrylamide neomycin B. The addition of the acrylamide–aminoglycoside had no observable effect on gel polymerization. As a control, we also prepared gels embedded with either paromomycin or neomycin B [22].

RNA binding to the cross-linked acrylamide–aminoglycoside was analyzed using the interaction of the TSMC RNA with aminoglycoside molecules as a model system [5,22,24]. The interaction of the TSMC RNA with paromomycin was previously characterized by ITC methods [24]. In all cases where an aminoglycoside is present, the mobility of the RNA is greatly reduced compared with the gel run in the absence of ligand (Figs. 4–6). Thus, the gels containing cross-linked paromomycin show that RNA mobility is significantly reduced compared with the embedded paromomycin (Figs. 4 and 6). Similarly, the gels containing cross-linked neomycin B show decreased RNA mobility compared with the embedded neomycin B (Figs. 4 and 6). This decreased migration indicates that binding is occurring in the gel between the RNA and the aminoglycoside and that cross-linking the aminoglycoside to the acrylamide results in a significant decrease of RNA mobility compared with the embedded ligand.

The TSMC RNA interacted with the cross-linked aminoglycosides to produce quantifiable data. We analyzed this interaction by measuring the relative migration (R_r) of the TSMC RNA against the bromophenol blue internal standard and plotting the R_r value against the concentration of cross-linked and embedded paromomycin and to the concentration of cross-linked and embedded neomycin B (Fig. 5). Plotting of the reciprocal relative migration ($1/R_r$) against the concentration of cross-linked paromomycin and against the concentration of cross-linked neomycin B (Fig. 6A and B) generated straight lines, from which the corresponding average apparent dissociation constants were determined from the inverse of the slope of the lines [25]. From the data in Fig. 6, we calculated an average apparent K_d value of 156 ± 7 μM for TSMC RNA binding cross-linked paromomycin and an average apparent K_d value of 450 ± 31 μM for TSMC RNA binding cross-linked neomycin B. In comparison, the use of embedded ligands provides much less reliable quantification (particularly at low concentrations of the embedded product) because a straight line does not result when plotting $1/R_r$ versus aminoglycoside concentration (Fig. 6C and D).

Discussion

We have used affinity electrophoresis coupled with cross-linking of the ligand to the gel matrix to quantitatively study RNA–aminoglycoside interactions. Previously, using only embedded ligands, we showed that binding occurred in a dose-dependent manner. However, when plotting $1/R_r$ values versus ligand concentration, we did not get a straight line with the embedded ligands [22] (Fig. 6C and D). This prevented binding from being quantified with high accuracy. We attributed this nonlinearity to the ligand moving in the gel during electrophoresis. Here, we overcame this limitation by cross-linking the aminoglycoside directly to the gel by reacting the aminoglycoside with acryloyl chloride. During gel polymerization, the ligand becomes covalently attached to the gel. Using this method, the TSMC RNA that interacts with the aminoglycoside binds significantly tighter to the cross-linked ligand than to the embedded ligand, and binding approaches saturation at the higher ligand concentrations examined (Fig. 5). To the best of our knowledge, this is the first example of cross-linking of a small molecule ligand to the polyacrylamide gel to study RNA–small molecule interactions.

Using the cross-linked aminoglycosides, we can determine an average apparent K_d value for the RNA–ligand interaction (Fig. 6). We use the term average apparent K_d because when we react the acryloyl chloride with the aminoglycoside, we get a mixture of products in which the acryloyl groups potentially react with each alcohol and amino group. Rings I and II on the aminoglycoside (Fig. 1) are the rings that most closely interact with the RNA [26]. When the acryloyl group reacts with alcohol or amine groups on ring I or II, binding will be obstructed and the average apparent K_d value will be increased compared with when the acryloyl reacts at ring III or IV. This mixture of products, with some products binding more weakly than others, results in the measured average apparent K_d being weaker (156 ± 7 μM) than what was previously measured in solution (0.6 μM [5]). However, this does not take away from our main conclusion that using the cross-linked aminoglycoside results in quantifiable data, as shown by the linear plots in Fig. 6. We note that the difference between our affinity electrophoresis determined K_d value measured here and the previously reported value found in solution could also reflect differences in temperature and buffer composition between these methods.

The average apparent K_d values showed tighter binding for the cross-linked paromomycin than for the cross-linked neomycin B (Fig. 6). Although binding of neomycin B to the TSMC RNA used here has not been demonstrated previously, the binding of neomycin B to a similar C–C mismatch was shown to be tighter than that of paromomycin. This apparent discrepancy is likely due to the fact that neomycin B has more amino groups in ring I than does paromomycin (Fig. 1). As the pK_a of the amino group is lower ($pK_a \sim 9$–10) than that of the hydroxyl group ($pK_a \sim 16$–17), the one equivalent of sodium bicarbonate will preferentially deprotonate the amino to form a reactive amine with an available lone pair that immediately reacts with acryloyl chloride. Because neomycin B contains more amine groups at ring I, reaction with acryloyl chloride reduces the ligand binding ability of neomycin B for the TSMC RNA to a greater extent than it does for paromomycin.

This method was used primarily to quantify RNA–aminoglycoside interactions; however, it should be possible to apply this method to any ligand that binds RNA as long as the cross-linked ligand does not interfere with gel polymerization. In addition, our cross-linked ligand affinity electrophoresis method is particularly useful for comparing interactions between different RNA molecules with the same aminoglycosides by running a constant concentration of each RNA on the same gel.

In summary, we have shown that an affinity electrophoresis-based method can be made quantifiable for determining dissociation constants of RNA–aminoglycoside interactions. This method can easily be applied to other RNA–small molecules using equipment and reagents common to most laboratories. Furthermore, synthesis of other cross-linked aminoglycosides and subsequent testing to different RNA molecules of various sequences and sizes can also be achieved following our method to obtain quantitative binding information.

Acknowledgment

We thank current and past members of the Johnson laboratory for useful discussions. This research was supported by grants from the Natural Sciences and Engineering Research Council of Canada (P.E.J. and M.G.O.) and by the National Institute of General Medical Science (Center in Chemical Methodologies and Library Development at the University of Kansas, KU-CMLD, NIH P50 GM069663, NIH P41-GM076302) and the Ontario Centres of Excellence (OCE) to M.G.O.

References

[1] R.K. Montange, R.T. Batey, Riboswitches: emerging themes in RNA structure and function, Annu. Rev. Biophys. 37 (2008) 117–133.
[2] A. Roth, R.R. Breaker, The structural and functional diversity of metabolite-binding riboswitches, Annu. Rev. Biochem. 78 (2009) 305–334.
[3] G. Mayer, The chemical biology of aptamers, Angew. Chem. Int. Ed. 48 (2009) 2672–2689.
[4] S. Magnet, J.S. Blanchard, Molecular insights into aminoglycoside action and resistance, Chem. Rev. 105 (2005) 477–497.
[5] J.B.-H. Tok, J. Cho, R.R. Rando, Aminoglycoside antibiotics are able to specifically bind the 5′-untranslated region of thymidylate synthase messenger RNA, Biochemistry 38 (1999) 199–206.
[6] Y. Tor, Targeting RNA with small molecules, ChemBioChem 4 (2003) 998–1007.
[7] C.S. Chow, F.M. Bogdan, A structural basis for RNA–ligand interactions, Chem. Rev. 97 (1997) 1489–1513.
[8] J.R. Thomas, P.J. Hergenrother, Targeting RNA with small molecules, Chem. Rev. 108 (2008) 1171–1224.
[9] F. Aboul-Ela, Strategies for the design of RNA-binding small molecules, Future Med. Chem. 2 (2010) 93–119.
[10] R.W. Carthew, E.J. Sontheimer, Origins and mechanisms of miRNAs and siRNAs, Cell 136 (2009) 642–655.
[11] H. Siomi, M.C. Siomi, On the road to reading the RNA-interference code, Nature 257 (2009) 396–404.
[12] P.A. Sharp, The centrality of RNA, Cell 136 (2009) 577–580.
[13] K. Karns, J.M. Vogan, Q. Qin, S.F. Hickey, S.C. Wilson, M.C. Hammond, A.E. Herr, Microfluidic screening of electrophoretic mobility shifts elucidates riboswitch binding function, J. Am. Chem. Soc. 135 (2013) 3136–3143.
[14] L.M. Hellman, M.G. Fried, Electrophoretic mobility shift assay (EMSA) for detecting protein–nucleic acid interactions, Nat. Protoc. 2 (2007) 1849–1861.
[15] K.T. Gagnon, E.S. Maxwell, Electrophoretic mobility shift assay for characterizing RNA–protein interaction, Methods Mol. Biol. 703 (2011) 275–291.
[16] V. Horejsi, Affinity electrophoresis, Anal. Biochem. 112 (1981) 1–8.
[17] K. Takeo, Affinity electrophoresis: principles and applications, Electrophoresis 5 (1984) 187–195.
[18] P. Tomme, A. Boraston, J.M. Kormos, R.A.J. Warren, D.G. Kilburn, Affinity electrophoresis for the identification and characterization of soluble sugar binding by carbohydrate-binding modules, Enzyme Microb. Technol. 27 (2000) 453–458.
[19] C.D. Cilley, J.R. Williamson, Analysis of bacteriophage N protein and peptide binding to boxB RNA using polyacrylamide gel coelectrophoresis (PACE), RNA 3 (1997) 57–67.
[20] J.M. Kormos, P.E. Johnson, E. Brun, P. Tomme, L.P. McIntosh, C.A. Haynes, D.G. Kilburn, Binding site analysis of cellulose binding domain CBD_{N1} from endoglucanase C of *Cellulomonas fimi* by site-directed mutagenesis, Biochemistry 39 (2000) 8844–8852.
[21] N.H.H. Heegaard, Affinity in electrophoresis, Electrophoresis 30 (2009) S229–S239.
[22] S.N. Boodram, C.M. Cho, T.J. Tavares, P.E. Johnson, Identification of RNA–ligand interactions by affinity electrophoresis, Anal. Biochem. 409 (2011) 54–59.
[23] J.F. Milligan, D.R. Groebe, G.W. Witherell, O.C. Uhlenbeck, Oligoribonucleotide synthesis using T7 RNA polymerase and synthetic DNA templates, Nucleic Acids Res. 15 (1987) 8783–8798.
[24] T.J. Tavares, A.V. Beribisky, P.E. Johnson, Structure of the cytosine–cytosine mismatch in the thymidylate synthase mRNA binding site and analysis of its interaction with the aminoglycoside paromomycin, RNA 15 (2009) 911–922.
[25] K. Takeo, Advances in affinity electrophoresis, J. Chromatogr. A 698 (1995) 89–105.
[26] Q. Vicens, E. Westhof, Crystal structure of paromomycin docked into the eubacterial ribosomal decoding A site, Structure 9 (2001) 647–658.